ICONHIC 2016
1st International Conference on Natural Hazards & Infrastructure
28-30 June, 2016, Chania, Greece

A simplified method for the analysis of embedded footings accounting for soil inelasticity and foundation uplifting

A. Kladis[1], F. Gelagoti
National Technical University of Athens

N. Laourakis[2]
Arup, Advanced Technology & Research Department, London

I. Anastasopoulos
ETH, Zurich

ABSTRACT

The paper introduces a simplified methodology for the analysis of rocking SDoF systems founded on slightly embedded foundations. Following a comprehensive numerical study on the static and dynamic response of square footings with varying embedment ratios, a set of non-linear springs and dashpots is extracted accounting for soil-foundation interaction phenomena. To test the effectiveness of the proposed methodology, the dynamic response of the proposed spring model is compared against that of a rigorous 3D FE model for a variety of earthquake excitations. It is concluded that for all test cases the spring model predicts quite accurately the maximum foundation rotation and the maximum acceleration at the center of mass of the oscillator, but tends to underestimate the actual accumulated settlement. Nonetheless, the accuracy of the proposed methodology increases for low-medium intensity events and moderately-lightly loaded systems.

Keywords: embedded footing, simplified methodology, seismic, soil-structure interaction, non-linear springs

INTRODUCTION

One of the most popular methods to engineering practitioners for modeling soil-foundation-structure interaction problems is the beam-on-Winkler Foundation (BWF) approach (basically due to its simplicity, minimal computational effort and ease of implementation). The idea dates back to 1867 and indicates that the physical soil stratum may be replaced by a system of continuously distributed springs along the foundation width. The BWF method has been widely involving over the last 30 years, from the early work of Chopra and Yim (1984) on the rocking response of linear structures on elastic soil, to the recent sophisticated models of Allotey & Naggar (2007) and Raychowdhury & Hutchinson (2009) that may account for strongly non-linear effects (i.e. soil yielding, foundation uplifting-sliding etc.).

This paper introduces an alternative to the BWF approach; a simplified analysis methodology (originally proposed by Anastasopoulos et al, 2013) in which the soil is replaced by concentrated springs and dashpots (a horizontal, a vertical and a rotational). The proposed methodology is ideally implemented to slightly embedded

[1] Corresponding Author: Civil Engineer, MSc, National Technical University of Athens, *email: anthony.kladis@gmail.com*
[2] Structural Engineer, MEng, Arup London; formerly National Technical University of Athens
email: nicklaourakis@gmail.com

footings experiencing severe (seismic) moments and may account for complex soil-foundation interaction effects.

METHODOLOGY

The proposed methodology is applied to a single degree of freedom (SDoF) system of height h, carrying a concentrated mass *m*, founded on a square embedded foundation of width *B a*nd depth *D*. The h/B ratio is assumed constant at 1.2, while D/B takes values 0.4, 0.7 and 1. As for the soil properties, the SdoF lies on a clay stratum of depth z, with undrained shear strength S_u = 150 kPa, shear wave velocity V_S = 227 m/sec, and density $\rho = 2\ t_n/m^3$. In order to concentrate on the nonlinear response of the foundation, the oscillator is assumed to be rigid.

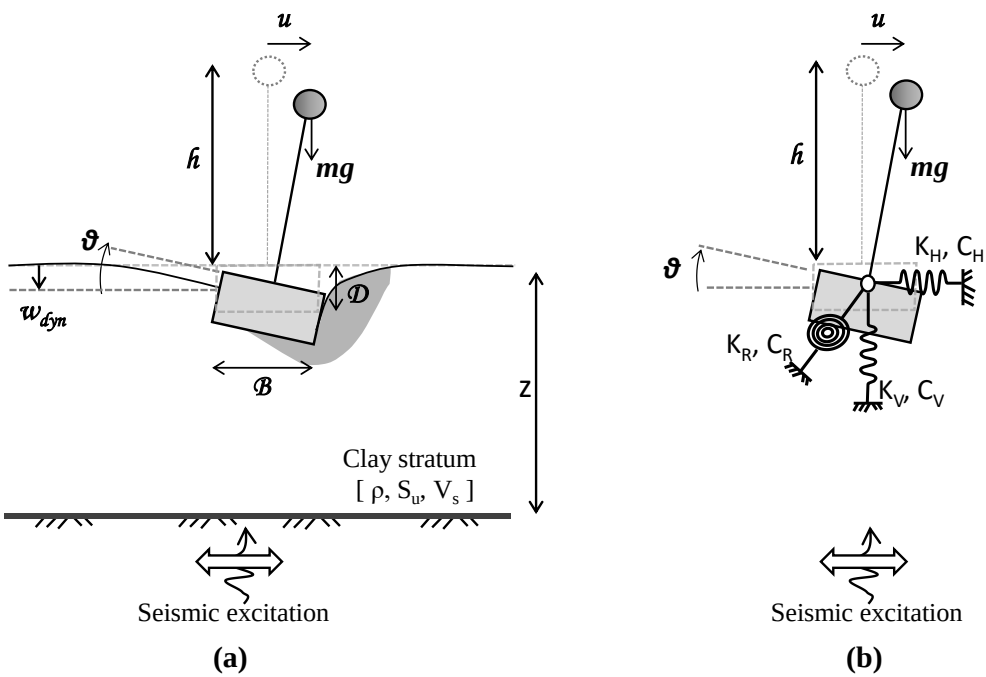

Figure 1: Problem definition: (a) the rigorous approach: the entire soil-foundation-structure system is modelled; and (b) the proposed simplified method where the soil-foundation system is replaced by springs K_R K_V, K_H accompanied by linear dashpots C_R, C_V, and C_H.

A schematic view of the problem under study is illustrated in Fig.1; the example SdoF under the seismic action tends to rock upon its foundation. This rocking motion induces plastic deformations on the supporting ground (rotations and settlements) which ultimately modify the transmitted motion to the oscillator. Scope of this study is to replace this complex soil-foundation system (with all its interactions) by a set of properly calibrated springs and dashpots (as in Fig.1b).

Since the problem under study is rocking-dominated (due to the slenderness of the envisioned superstructural system), the horizontal (K_H and C_H) and vertical (K_V and C_V) springs and dashpots will be assumed to behave elastically following the published solutions for embedded footings by *Gazetas et al (1983*). On the contrary, for the simulation of the rotational degree of freedom a *nonlinear (rotational) spring* accompanied by a linear dashpot are implemented. To define the nonlinear K_R and C_R two (2) relations are required (both of them being a function of the embedment ratio D/B and the factor of safety against vertical loading F_S): (a) the moment–rotation relation (M–θ) to formulate the nonlinear rotational spring K_R and **(b)** the damping coefficient–rotation relation (C_R–θ) for the definition of the rotational dashpot C_R.

Furthermore, to simplistically account for the accumulation of settlement under the rocking footing, the dynamic settlement–rotation (Δw_{dyn}–θ) relation is required. All these three relations (M–θ, C_R–θ and Δw_{dyn}–θ) are derived from rigorous 3D FE non-linear analysis of the entire soil-foundation system, as will be explained in the ensuing. The M–θ relation is computed on the basis of displacement-controlled monotonic pushover analyses, whereas cyclic pushover analyses are conducted to derive the C_R–θ and Δw_{dyn}–θ relations.

Estimation of the Rotational Impedances K_R and C_R

The 3D FE model comprises of the entire soil–foundation–structure system considering material and geometric nonlinearities. As illustrated in Fig.2, taking advantage of problem symmetry, only half of the soil–foundation–structure system is modeled to reduce the computational cost. The oscillator (bridge pier) is modeled with elastic (practically rigid) beam, while the deck mass is represented by a concentrated mass element on top of the pier. The footing is modeled with elastic (8-node) solid elements, while continuum nonlinear solid elements are used for the simulation of soil. The latter, obey to a nonlinear kinematic hardening model, with a Von Mises failure criterion with associated flow rule (*Anastasopoulos et al, 2011*). Special contact elements are introduced at the soil–foundation interface, permitting detachment-sliding between the footing and the supporting soil.

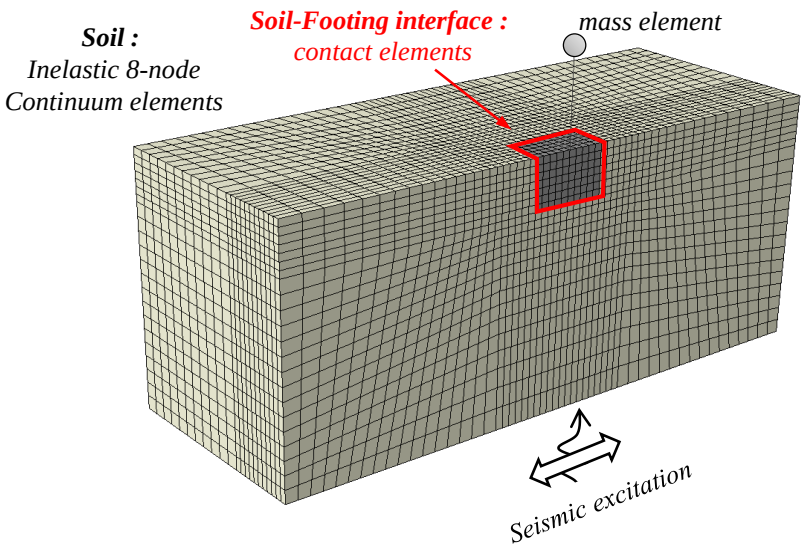

Figure 2: The Rigorous 3D finite element model.

The M–θ curves are computed through displacement-controlled monotonic pushover analyses, utilizing the FE model of Fig.2. The same procedure is followed for all three ratios of embedment D/B=0.4, 0.7 & 1 and for each depth ratio, the P-O analysis is conducted for three distinctive factors of safety against vertical loading (i.e., F_S =2, 5 and 10). Static factors of safety $F_S < 2$ are rarely applied in practice (to limit excessive settlements), and are therefore not considered herein. On the other hand, for $F_S > 10$, soil inelasticity is very limited and the rocking response of footing may be considered practically elastic. An illustrative view of the computed M-θ curve is portrayed in Fig.3a. Three characteristic regions (representing different foundation performances) shall be identified: (a) a quasi-elastic response of a constant rotational stiffness K_{R0} (evident for $\theta < \theta_o$ rad), (b) a plastic response (for large rotations θ when the ultimate foundation capacity is reached) and (c) an intermediate region covering the area between the quasi-elastic and the plastic region.

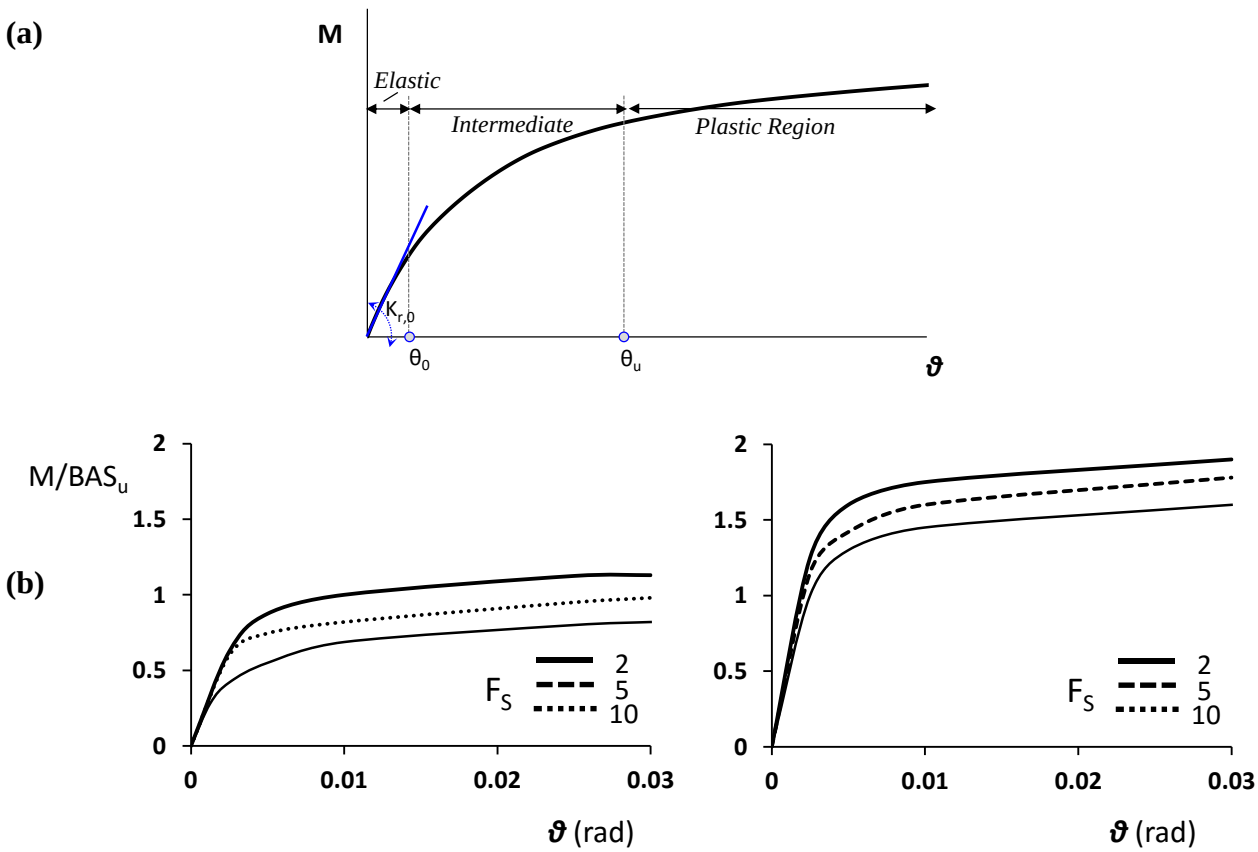

Figure 3. (a) Example of a typical M-θ curve (b) Computed M-θ curves for three different F_s for an embedded footing with D/B=0.4 (left) and D/B=1 (right).

The Quasi Elastic Response: Estimation of $K_{r,0}$

In Fig.4a, the evolution of $K_{r,0}$ as a function of safety factor F_S and the embedment ratio D/B = 0, 0.4 & 1 is displayed. Quite surprisingly the shallow and the embedded footings do not follow the same pattern. In case of no embedment, the $K_{r,0}$ keeps increasing with increasing Fs. Naturally large Fs values come with minimal soil plastifications, which is accompanied by higher resistance to the experienced lateral thrust. However, for D/B≠0 the $K_{r,0}$ is peaking at a specific Fs value, termed herein $F_{S,Crit,}$ and after that point tends to decrease at a quite smooth rate. Besides, it was found that this critical value of F_S decreases as the depth of embedment increases according to Eq (1).

$$F_{S,Crit} = -3\ {}^{D}/_{B}\ + 6 \tag{1}$$

A schematic insight on the mechanics governing this peculiar response is portrayed in Fig.4b. Two distinctive trends shall be identified: (i) the $K_{r,0}$ (as in the case of the shallow footing) increases as the soil plastification in the surrounding soil tends to decrease (top Figures); (ii) the $K_{r,0}$ decreases as the intensity of the 'trench' effect decreases (bottom Figures). Evidently, in the latter case at low F_S values (i.e case of heavily loaded foundation) the soil around the footing tends to displace inwards. This 'restricted' soil movement increases the lateral soil pressure and in turn produces higher rotational resistance. To account for all the above phenomena, a two-branch Equation (2,3) is suggested for the definition of $K_{r,0}$ as a function of embedment ratio D/B and factor of safety F_S.

$$K_{R0} = \frac{K_{R,Gazetas}}{1+{}^{D}/_{B}} \begin{cases} -0.05\,F_S{}^2 + 0.36\,F_S + {}^{D}/_{B} & F_S \le F_{S,\,Crit} \quad (2) \\ {}^{D}/_{B}\ \left(1 - {}^{F_S}/_{20}\right) + 0.7 & F_S \ge F_{S,\,Crit} \quad (3) \end{cases}$$

where $K_{R,Gazetas}$ is the elastic rotational stiffness of a shallow square footing given by:

$$K_{R,Gazetas} = \frac{3.6\,G\,(B/2)^3}{1-\nu}\left\{1 + 1.26\,\frac{D}{B/2}\left(1 + \frac{D}{B/2}\right)\right\} \tag{4}$$

where G is the small strain shear modulus of soil and ν the Poisson's ratio.

The Plastic and Intermediate Response: Determination of the Ultimate Moment Capacity

As evidenced in Fig.3b, plastic response (for all embedment ratios examined) starts approximately at a footing rotation of around 0.01 rad. At that value the foundation has already reached its ultimate moment capacity. The latter may be expressed as a function of embedment depth D/B and factor of safety F_S following Eq (5).

$$\frac{M_{ult}}{B^3 Su} = \left[\left(\frac{D}{B}\right)^2 - 0.17\frac{D}{B} + 0.84\right](-0.03F_S + 1) \tag{5}$$

The intermediate region, on the other hand, is the region bridging the quasi-elastic and plastic response. If the soil behaved as an ideally elastic–plastic material, there would be no need to consider and calibrate this intermediate phase of response. Just the previously described solutions would be enough to completely define the M–θ relation. However, the soil– foundation system behaves strongly non-linearly long before reaching its ultimate capacity. Hence, the need of defining this "connecting" area is vital. Referring back to Fig.3b, it becomes clear that the initiation of this intermediate branch is not unique for all embedded systems, but differs with respect to the D/B ratio and factor of safety F_S. As F_S increases, the appearance of the intermediate region is delayed, whilst as the depth ratio increases, the lateral soil tends to hold back the footing, suspending the initiation of a highly non-linear performance. In an attempt to combine all these phenomena into one single expression, Eq (6) correlates θ_s (i.e. the value of rotation angle at which M-θ curve departs from the elastic range and starts behaving non-linearly) to D/B and F_S as follows:

$$\theta_S = \frac{N\,B}{4\,K_{R0}}\left[1.29\left(\frac{D}{B}\right)^2 - 2.16\left(\frac{D}{B}\right) + 1\right]\left(\frac{1}{F_S}\right)^{0.75(D/B)^2 + 1.68(D/B)} \tag{6}$$

where $K_{r,0}$ is the initial quasi-elastic rotational stiffness, as described previously. Despite its complexity, it is worthwhile to observe that for D/B=0 Eq.6 reduces to the formula proposed by Anastasopoulos et al. (2013) for surface footings.

By normalizing the M–θ curves of Fig.3b to $M/M_{ult}=f\,(\theta/\theta_S)$ (following Eq. 5 and 6), we may end up with one single non-dimensional curve (Fig.5) for each embedment ratio D/B.

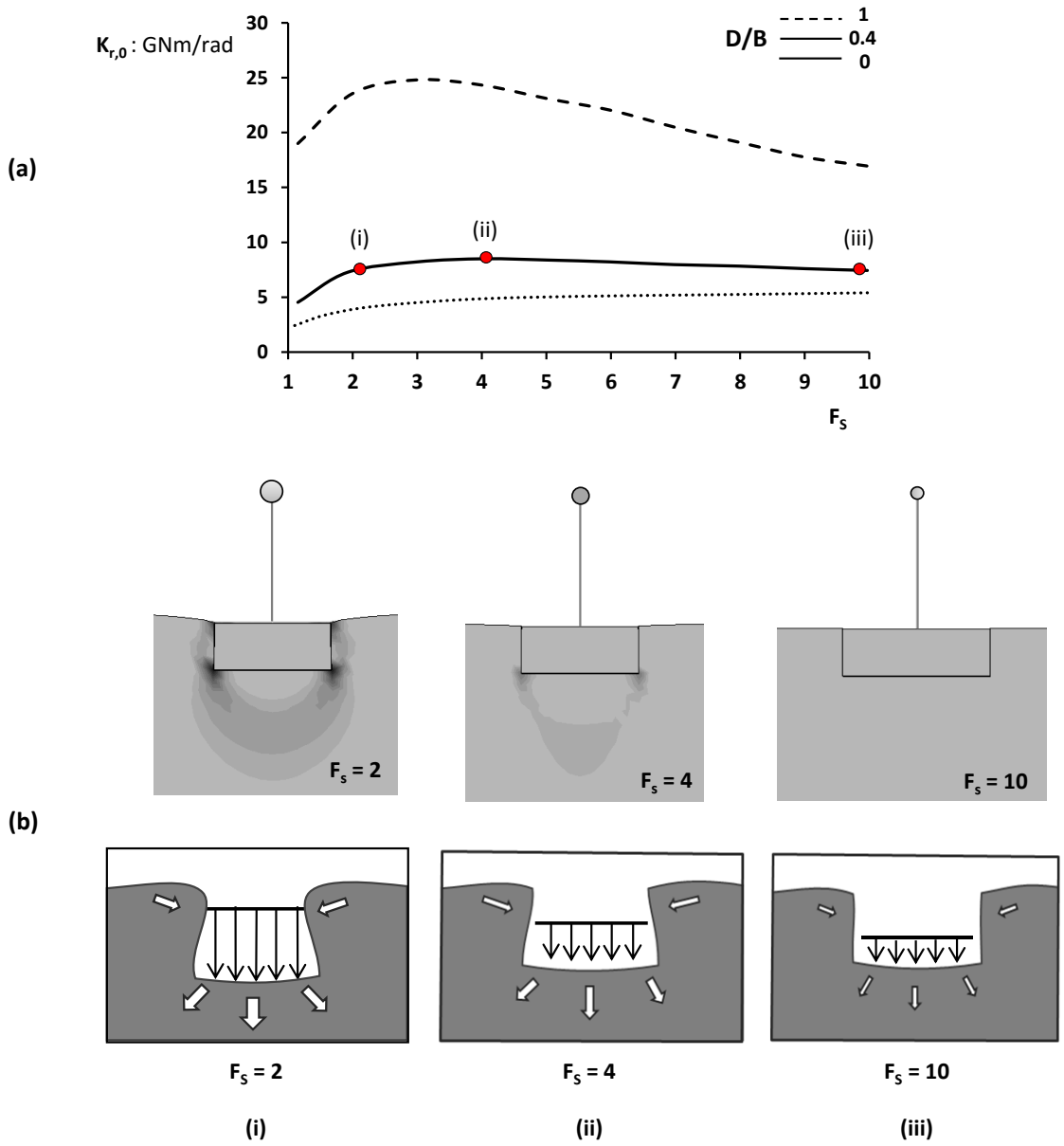

Figure 4: (a) Initial rotational stiffness K_{R0} as a function of FS; (b) embedded footing (D/B=0.4) subjected to vertical loading: Snapshots of deformed mesh with superimposed plastic strain contours for: F_S=2, 4 and 10, just before the Push-over (top plots) and schematic view of the trench effect for different F_S values (bottom).

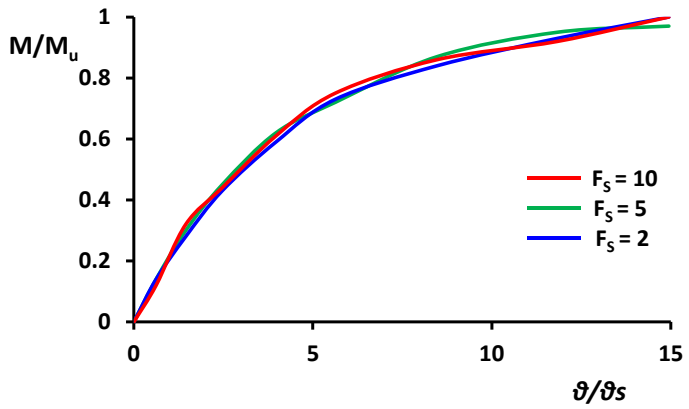

Figure 5. A unique non-dimensional Moment-Rotation relation for FS=2-10. Results correspond to an embedded footing of D/B=0.4

Estimation of the rotational dashpot C_R

The hysteretic rotational damping is computed on the basis of displacement-controlled cyclic pushover analysis, utilizing the 3D FE model of Fig.2. The rotational damping coefficient C_R of a simplified SDoF model is assumed to be a function of the effective (secant) rotational stiffness $K_{r,0}$, the hysteretic damping ratio ξ and a characteristic frequency ω, according to Eq (7).

$$C_R = \frac{2\,K_{R0}\xi}{\omega} \tag{7}$$

The hysteretic damping ratio ξ is computed by the area of the M–θ loops of the cyclic pushover. As for the angular frequency $\omega = 2\pi/T$, this term is also a function of rotation; as rotation increases the effective period T of the rocking system increases. However, in order to maintain the simplicity of this methodology and following the recommendation of Anastasopoulos et al. (2013), T is assumed constant and equal to the initial natural period $T_{n,0}$ (at θ=0) of the rocking system. The latter is estimated as:

$$T_{n,0} = 2\pi\sqrt{\frac{m\,h^2}{K_{r,0} - mgh}} \tag{8}$$

where $K_{r,0}$ is the initial rotational stiffness, m the total mass of superstructure and h the pier height.

The derived C_R–θ curves (for our example test cases) are depicted in Fig.6. Evidently a non-linear dashpot would ideally be required. The C_R coefficient is peaking for footing rotations between 10^{-5} – 10^{-3} rad, while it decreases as the F_S increases. To simplify things further, C_R is assumed constant with θ and equal to its local maxima.

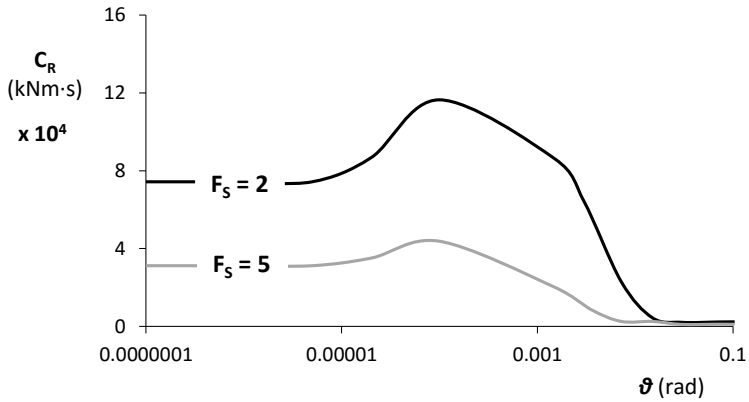

Figure 6: Evolution of damping coefficient C_R with foundation rotation θ. Results correspond to an embedded footing of D/B=0.4

Approximation of the accumulated footing settlement

As explained previously, the proposed spring model is inherently incapable to capture the accumulation of footing settlement. To overcome this weakness, the dynamic settlement time history is approximated on the basis of a parallel computation procedure originally suggested by Anastasopoulos et al. (2013). Namely:

(a) First the rotation time history ϑ(t) is calculated (using the simplified spring model).
(b) In the next step, the graph of the rotation time history ϑ (t) is divided into a number of half-cycles ϑ_i.
(c) For each half-cycle of amplitude ϑ_i, the expected settlement Δw_i is computed by means of an algebraic formulation that correlates rotation amplitude θ to settlement Δw (as described in the ensuing).
(d) Finally the entire settlement time-history is constructed by adding the settlement of each half-cycle to the previous one.

Δw–θ formulation

To estimate the accumulation of settlement with footing rotation, the embedded footings of varying F_S are imposed to displacement-controlled cyclic pushover analyses of gradually increasing amplitude, as illustrated in Fig. 7a. An example output of this type of analyses is depicted in Fig.7b (corresponding to a square embedded foundation of D/B=0.4 and F_S=2). By extracting the accumulated settlement Δw per loading cycle, the plot of Fig.8 is computed that correlates the amplitude of footing rotation θ to the per cycle accumulated settlement Δw (normalized to the foundation width B). Naturally, the footing of F_S=2 tends to sink under this rocking movement, and as such accumulates much higher settlements than the footing of F_S=10 that demonstrates a predominantly rocking response with only minimum settlement. Eq. 9 aims to concentrate all the above trends in one single expression (which is unique for all examined depth ratios) as follows:

$$\frac{\Delta w}{B} = -\left[(1.67F_S - 9.2)\theta^2 + \frac{2.54}{F_S{}^{2.6}}\theta\right] \tag{9}$$

The reader is encouraged to note that the proposed parabolic equation underestimates the cyclic settlement of F_S=3 for foundation rotation θ greater than 0.025 rad (an unrealistically high foundation rotation), while for heavily loaded systems (F_S=2), where settlements are important, the formula describes closely the actual footing response.

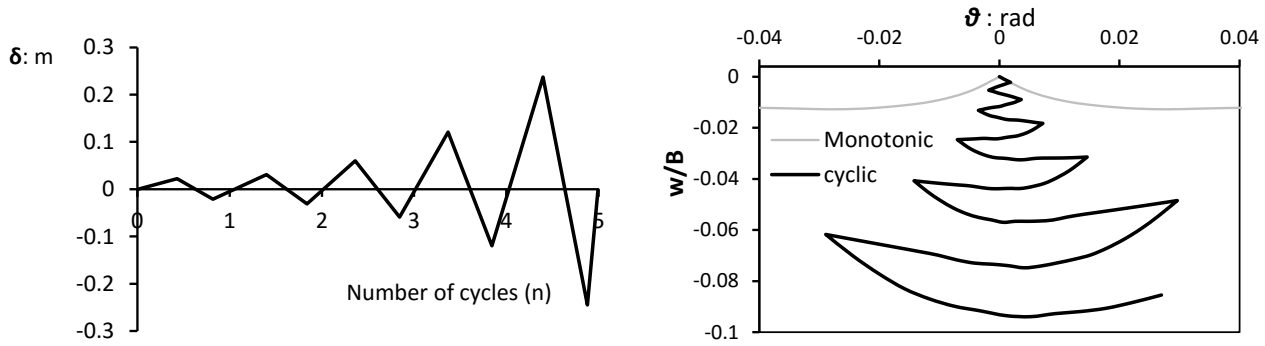

Figure 7. Footing subjected to a cyclic pushover loading: (a) displacement-controlled loading protocol; (b) normalized settlement (w/B) – rotation (θ) loops. (Example refers to a footing of D/B=0.4 and F_S = 2).

SEISMIC RESPONSE OF THE ROCKING FOOTING: VALIDATION AND INSIGHTS

Having established the key components of our simplified model, the numerical predictions of the latter will be compared with those produced by a rigorous 3D FE model. As for the parameters of our example test case, a SDoF system of height h=6m, B=5m and D=2m is assumed, lying on clay stratum of undrained shear strength S_u=150 kPa. Two loading Scenarios are examined for a heavily loaded system with factor of Safety F_S=2.

The slender SDoF system is subjected to the recording of the recent Kefalonia2014 earthquake (with a PGA at 0.73g) and to the Bolu time-history recorded during the famous Duzce1999 earthquake (with PGA at 0.8g). The seismic performance is displayed in Fig.9 for both events. Evidently, the system performs nonlinearly. The strong main pulse of the Bolu event provokes higher rotations, while the Kefalonia motion, although producing lower θ values, eventually yields higher settlement.

As for the predictions of the simplified model (gray line), in both earthquake scenarios the estimation of the experienced acceleration at the center of mass as well as the maximum foundation rotation is very good, while the spring model tends to underestimate the actual accumulated settlement. Note also, that in all cases the residual rotation of the spring model is zero; a condition that may be true for moderate earthquakes and high F_S, but is normally not satisfied when extensive soil nonlinearity is expected (case of low Fs and strong seismic shaking).

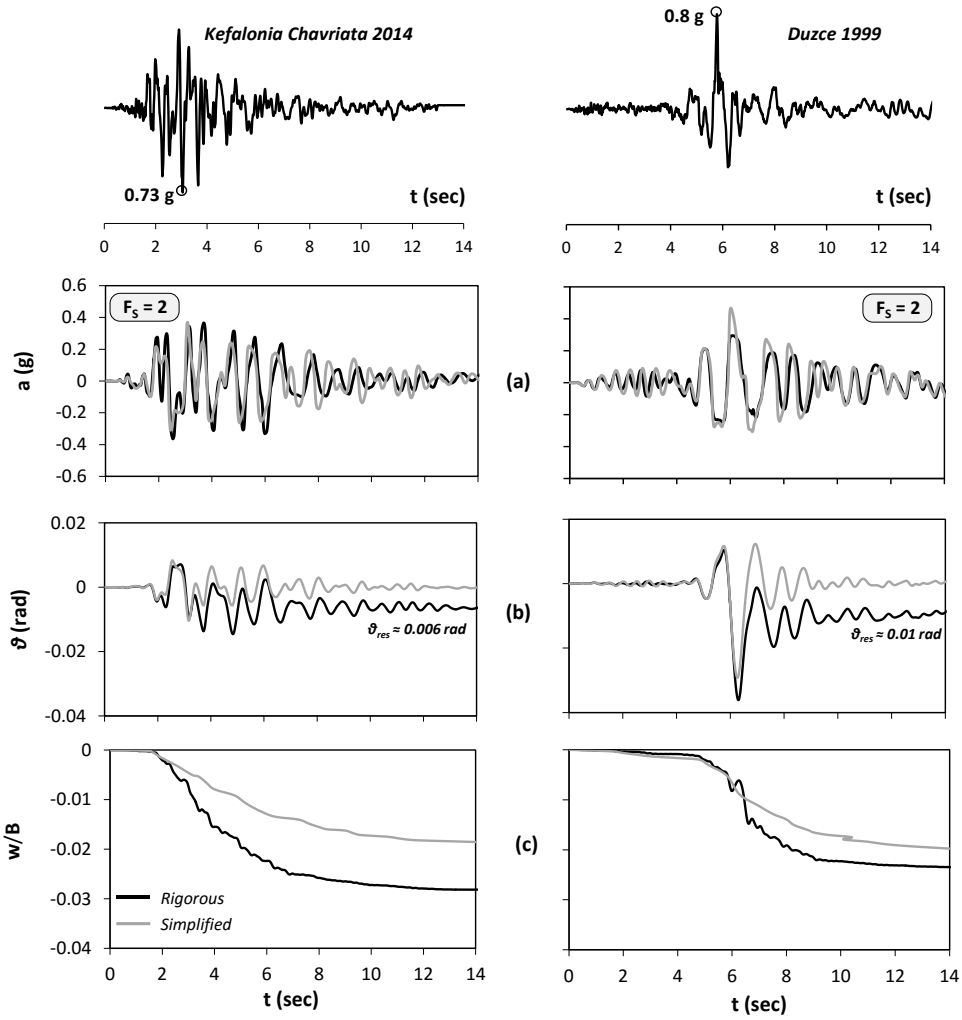

Figure 9. Rocking footing under strong seismic shaking. Comparison of the numerical prediction of the simplified model with the results of the rigorous 3D FE model. Results refer to a system with F_S = 2 and D/B=0.4 subjected to Chavriata 2014 (left column) and Duzce Bolu 1999 (right column): (a) acceleration time-history; (b) foundation rotation and (c) normalized foundation settlement.

Fig.10 portrays an overview of the performance of the spring model. The discrete points on the plots correspond to the six (6) different earthquake scenarios analysed. The top row exhibits the response of a heavily loaded system (with Fs=2), while the bottom row that of a normally loaded SdoF (with Fs=5). The comparison is presented in terms of maximum rotation θ_{max}, dimensionless residual settlement w_{res}/B and maximum acceleration a_{max} at the center of mass of the oscillator. It may be observed that for all test cases, the predictions of the simplified model are very good. Differences (with respect to the rigorous solution) are more pronounced in the extreme scenario of a heavily loaded structure (F_S=2), where the spring model fails to capture the residual rotation θ_{res}. As long as the intensity of the event remains low (e.g. Kalamata event) or as the F_S increases, the performance of the spring model is substantially improved.

CONCLUSIONS

The paper introduces a simplified analysis methodology to be implemented to slightly embedded footings experiencing severe (seismic) moments. The complex soil-foundation system is replaced by an appropriate set of springs and dashpots: linear elastic horizontal and vertical impedances K_H, C_H, K_V, C_V (following the published solutions for embedded footings by *Gazetas et al, 1983*) and a non-linear rotational spring K_R accompanied by a linear dashpot C_R. For the definition of K_R and C_R two relations are required (both of them

being a function of the embedment ratio D/B and the factor of safety against vertical loading F_S); the moment–rotation relation (M–θ) and the damping coefficient–rotation relation (C_R–θ). Furthermore, to simplistically account for the accumulation of settlement under the rocking footing, a dynamic settlement–rotation (Δw_{dyn}–θ) relation is introduced that approximates the foundation settlement as a function of the imposed foundation rotation. All these three relations (M–θ, C_R–θ and Δw_{dyn}–θ) are derived from rigorous 3D FE non-linear analysis of the entire soil-foundation system, and simplified formulas, have been derived. It is concluded that the proposed spring model, despite its several inherent approximations, seems to be sufficiently good for preliminary design purposes. The maximum accelerations and foundation rotations are accurately captured, while the residual settlement is nicely approximated.

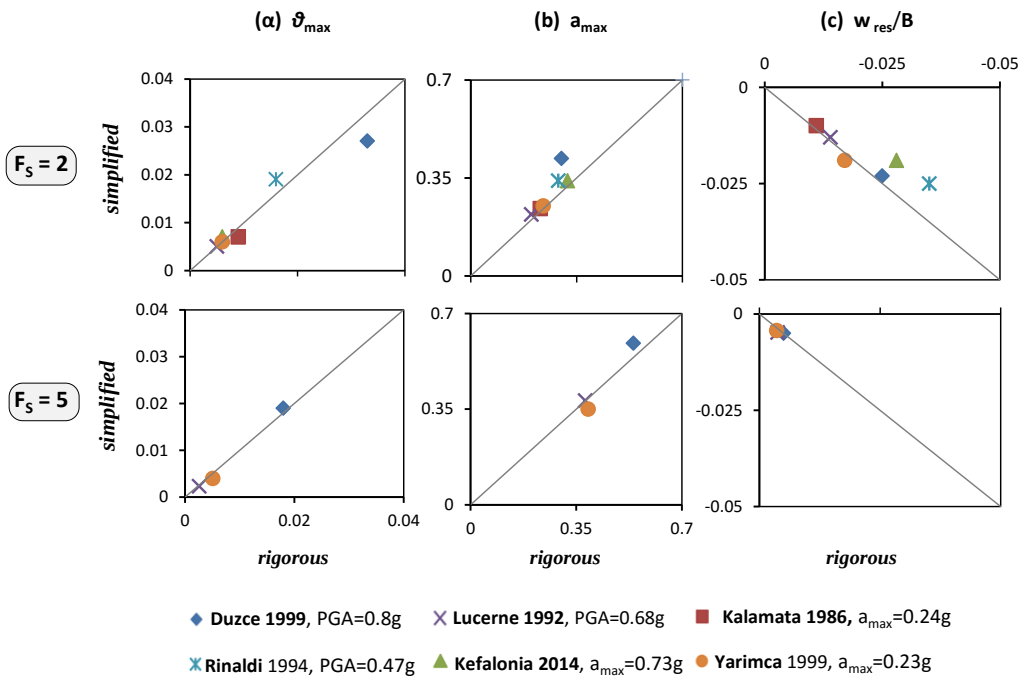

Figure 10. Overview of the performance of the spring model for six (6) earthquake scenarios: (a) maximum rotation θ_{max}; (b) maximum acceleration at the top of oscillator α_{max}; and (c) normalized residual settlement w_{res} /B.

REFERENCES

Allotey, N., & Naggar, MHE., (2007), "An investigation into the winkler modeling of the cyclic response of rigid footings", Soil Dynamics and Earthquake Engineering 2007; 28: 44–57.

Anastasopoulos I, Gelagoti F, Kourkoulis R, Gazetas G. Simplified Constitutive model for simulation of cyclic response of shallow foundations: validation against laboratory tests. Journal of Geotechnical and Geoenvironmental Engineering, ASCE 2011; 137 (12)1154–68

Anastasopoulos I, Kontoroupi Th. Simplified approximate method for analysis of rocking systems accounting for soil inelasticity and foundation uplifting; Elsevier; Soil Dynamics and Earthquake Engineering 56(2013) 28-43 ; 2013

Chopra, A.K. and Yim, S.C. (1984), "Earthquake Responses of structures with partial uplift on Winkler foundation", Journal of Sound and Vibration, 266(5): 957–965.

Gazetas G. Analysis of machine foundation vibrations: state of the art. Soil Dynamics and Earthquake Engineering 1983; 2:2–42

Gazetas G, Anastasopoulos I, Adamidis O, Kontoroupi T. Nonlinear rocking stiffness of foundations. Soil Dynamics and Earthquake Engineering 2013; 47: 83–91

Raychowdhury, P., & Hutchinson T., (2008). "Nonlinear Material Models for Winkler-Based Shallow Foundation Response Evaluation", Advances in Numerical and Computational Geotechnics, GeoCongress 2008: pp. 686-693.